



Contents lists available at ScienceDirect

Earth and Planetary Science Letters

journal homepage: [www.elsevier.com/locate/epsl](http://www.elsevier.com/locate/epsl)

## Measurement and implications of frequency dependence of attenuation

Ved Lekić<sup>a,\*</sup>, Jan Matas<sup>b</sup>, Mark Panning<sup>c</sup>, Barbara Romanowicz<sup>a</sup>

<sup>a</sup> Berkeley Seismological Laboratory, 225 McCone Hall, University of California, Berkeley, USA

<sup>b</sup> Laboratoire de Sciences de la Terre, CNRS-UMR 5570, Université de Lyon, Ecole normale supérieure de Lyon, 46, allée d'Italie, 69007 Lyon, France

<sup>c</sup> Department of Geological Sciences, 241 Williamson Hall, University of Florida, Gainesville, USA

### ARTICLE INFO

#### Article history:

Received 22 September 2008

Received in revised form 5 February 2009

Accepted 13 March 2009

Available online xxx

Editor: R.D. van der Hilst

#### Keywords:

seismic attenuation  
absorption band models  
normal modes

### ABSTRACT

Constraining the frequency dependence of intrinsic seismic attenuation in the Earth is crucial for: 1. correcting for velocity dispersion due to attenuation; 2. constructing attenuation and velocity models of the interior using datasets with different frequency contents; and, 3. interpreting lateral variations of velocity and attenuation in terms of temperature and composition. Frequency dependence of attenuation  $q$  can be represented by a power law  $q \propto q_0 \omega^{-\alpha}$ . Despite its importance, efforts at determining  $\alpha$  from surface wave and free oscillation data have been thwarted by the strong tradeoffs between the depth- and frequency dependence of attenuation. We develop and validate a new method that eliminates this tradeoff, allowing a direct estimation of effective frequency dependence of attenuation without having to construct a new depth-dependent model of attenuation. Using normal mode and surface wave attenuation measurements between 80 and 3000 s, we find that  $\alpha$  varies with frequency within the absorption band. It is 0.3 at periods shorter than 200 s, it decreases to 0.1 between 300 and 800 s, and becomes negative at periods longer than 1000 s.  
© 2009 Elsevier B.V. All rights reserved.

### 1. Introduction

As they propagate through the Earth, seismic waves experience attenuation and dispersion resulting from microscopic dissipative processes operating at a variety of relaxation times. These dissipative effects can be summarized by the macroscopic quantity  $q = -\Delta E / 2\pi E_{\max}$ , where  $\Delta E$  is the internal energy lost by a seismic wave in one cycle. This quantity can be related to the often-used quality factor  $Q$  through  $q \equiv (1/Q)$ . The Earth acts as an absorption band (e.g. Anderson, 1976) and attenuation depends on the frequency of oscillation. Within the absorption band, attenuation is relatively high and does not strongly depend on frequency. Outside the band, attenuation rapidly decreases with frequency. Since the relaxation times of the dissipative processes giving rise to the absorption band might strongly depend on pressure and temperature, the frequency bounds of the band can change with depth (e.g. Anderson and Minster, 1979; Minster and Anderson, 1981; Anderson and Given, 1982). Within the absorption band, the frequency dependence of  $q$  can be described using a power law,  $q \propto \omega^{-\alpha}$ , with a model-dependent  $\alpha$ , usually thought to be smaller than 0.5 (e.g. Anderson and Minster, 1979).

In the past few years, three new models of 3-D variations in upper mantle attenuation have been developed (Selby and Woodhouse, 2002; Gung and Romanowicz, 2004; Dalton and Ekström, 2006), offering the promise of clarifying the origin (thermal versus chemical)

of lateral heterogeneities. Yet, knowing the value of  $\alpha$  within the absorption band is required for interpreting lateral variations in attenuation in terms of temperature. It is also one of the governing parameters for interpreting observed lateral variations in seismic velocities. Matas and Bukowinski (2007) proposed a self-consistent attenuation model based on solid state physics and showed that anelasticity can substantially enhance seismic anomalies due to high temperature (by ~30%), thus confirming earlier observations of Romanowicz (1994). It is important to note that interpreting attenuation in terms of temperature and predicting its effects on seismic anomalies is only reasonable if the contribution of scattering is small compared to that due to intrinsic anelastic processes.

A non-zero  $\alpha$  implies that seismic waves of different frequencies are differently attenuated, and accordingly modifies the velocity dispersion relation. This has three important consequences: 1) because oscillations at different frequencies can have very different depth sensitivities to elastic and anelastic properties of the Earth, the value of  $\alpha$  affects the construction and interpretation of such profiles. In particular, the lower mantle  $q$  is mostly constrained by low-frequency modes and is thus not directly comparable to  $q$  obtained from high-frequency modes, which sample the upper mantle. A single radial attenuation profile is only relevant if  $\alpha = 0$ ; 2) because the frequency content of different attenuation measurements can differ, combining these datasets requires accounting for the effect of  $\alpha$ . For instance, if  $\alpha = 0.3$ , then  $q$  varies by a factor of two in a dataset including periods between 50 s and 5 s; 3) because geophysical datasets used to constrain Earth structure have very different dominant frequencies, using them together requires applying a

\* Corresponding author.

E-mail address: [leki@seismo.berkeley.edu](mailto:leki@seismo.berkeley.edu) (V. Lekić).

dispersion correction whose functional form is different for a non-zero  $\alpha$  than it is under the assumption of frequency-independent attenuation (Minster and Anderson, 1981).

Efforts at determining  $\alpha$  of the mantle have followed three approaches: theoretical studies, laboratory experiments and seismological observations. Theoretical investigations have focused on explaining the origin of the absorption band and incorporating models of likely relaxation mechanisms developed using solid state physics. Liu et al., (1976) and Kanamori and Anderson (1977) modeled the absorption band for a standard linear solid as a superposition of relaxation mechanisms, whose combined effects resulted in a frequency-independent  $q$  within the absorption band. Minster and Anderson (1981) applied insights from solid state physics to suggest that, for dissipation dominated by dislocation creep,  $\alpha > 0$  within the absorption band. Building on this work, Anderson and Given (1982) developed an absorption band model of the Earth in which the effects of pressure and temperature on the underlying relaxation mechanisms caused the frequency bounds of the band to change with depth.

Despite observational and experimental advances, no clear consensus concerning the value of mantle  $\alpha$  has emerged over the past 25 years. Nevertheless, theoretical predictions of  $\alpha > 0$  have been systematically confirmed in various laboratory studies. In their review paper, Karato and Spetzler (1990) argued that its value lies between 0.2 and 0.4. A more recent review by Romanowicz and Mitchell (2007) identifies a number of studies that collectively constrain  $\alpha$  to the 0.1–0.4 range. On the laboratory front, Jackson et al., (2005) obtained  $\alpha$  of  $0.28 \pm 0.01$  for a fine-grained olivine sample at a pressure of 300 MPa and temperature of 1200 °C. Relating laboratory measurements to  $\alpha$  in the real mantle, however, is not straightforward, due to uncertainties in extrapolating laboratory measurements to actual mantle materials under high-pressure and high-temperature conditions prevailing in the mantle.

On the other hand, seismological efforts at constraining globally-averaged  $\alpha$  within the absorption band have benefited from numerous measurements of surface wave or normal mode attenuation. Yet, although attenuation measurements of nearly 250 individual modes are currently available from the website of the Reference Earth Model project (<http://mahi.ucsd.edu/Gabi/rem.html>, see Fig. 1), the determination of  $\alpha$  has been confounded by the fact that oscillations at

different frequencies can have very different depth sensitivities to elastic and anelastic properties of the Earth. As a result of this tradeoff between frequency and depth effects, radial variations of attenuation can obscure the  $\alpha$  signal. The only studies attempting to obtain  $\alpha$  within the absorption band have found  $\alpha$  ranging from 0.1 to 0.3 while emphasizing the lack of resolution on the inferred values (Anderson and Minster, 1979; Anderson and Given, 1982; Smith and Dahlen, 1981). More recent studies (e.g. Shito et al., 2004; Cheng and Kennett, 2002; Flanagan and Wiens, 1998) have relied upon analysis of body waves to argue for values of  $\alpha$  in the 0.1–0.4 range. However, these studies were restricted to frequencies higher than 40 mHz and were of regional character, leaving unanswered the question of the average mantle  $\alpha$ .

A further complication in determining the frequency dependence of attenuation from seismic data arises from the discrepancy between attenuation measurements of spheroidal modes carried out using a propagating (surface) wave and those using a standing wave (normal mode) approach. As can be seen in Fig. 1, surface wave studies indicate attenuation values that are higher by about 15–20% than normal mode measurements of the same frequency. This discrepancy is not present in the toroidal modes. The origin of the discrepancy has not yet been determined. Durek and Ekström (1997) argued that noise can bias normal mode measurements toward lower attenuation values by up to 5–10%, Masters and Laske (1997) pointed to difficulties in choosing an appropriate time window for long-period surface waves as a reason for favoring normal mode measurements. A more recent study by Roullet and Clévédy (2000) based on a detailed analysis of measurement techniques and associated errors argues that the normal mode measurements are the more reliable. Yet, their analysis is far from being complete (Romanowicz and Mitchell, 2007), and the question of which set of measurements is more representative of the Earth's attenuation remains open. The compilation of attenuation measurements used in this study (Masters, personal communication) relies on careful windowing and a multi-taper approach in order to achieve a smooth transition from the normal mode values at lower frequencies to surface wave values at higher frequencies (see Fig. 1).

In light of the data uncertainties and the strong tradeoff between the depth- and frequency dependence of attenuation, seismic studies routinely focus on modeling the depth dependence of attenuation

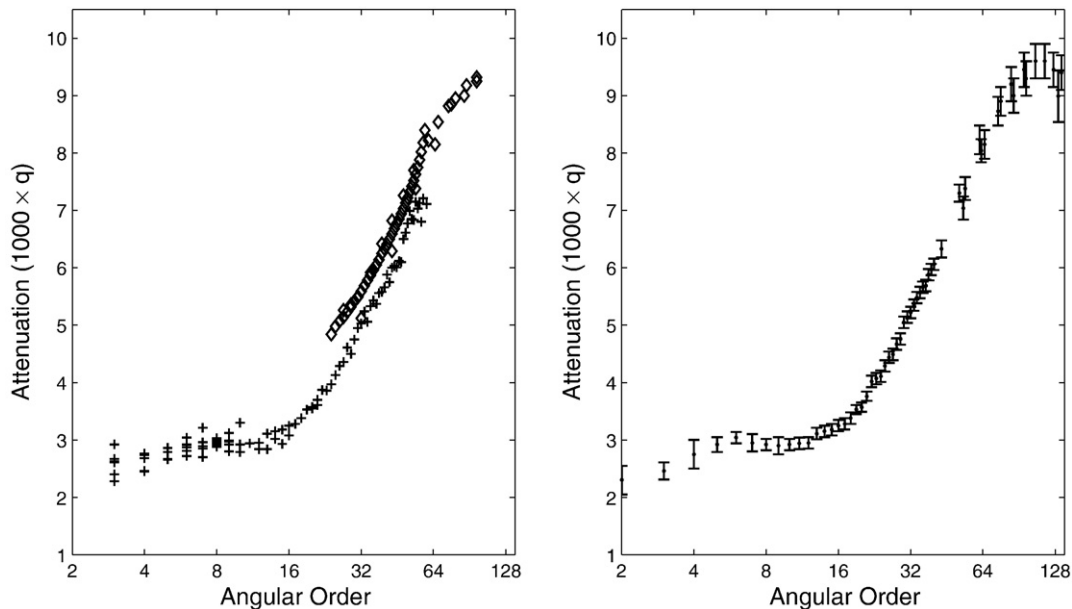


Fig. 1. Left: Attenuation measurements for the spheroidal fundamental mode branch (compilation from <http://mahi.ucsd.edu/Gabi/rem.html>). Measurements based on normal mode analysis (pluses) show attenuation values 15–20% smaller than corresponding surface wave-based measurements (circles). Right: The data compilation used in this study (Masters, personal communication) transitions smoothly from values more consistent with normal mode analyses at low frequencies to values consistent with surface wave analyses at higher frequencies.

(e.g. Anderson and Hart, 1978; Dziewonski and Anderson, 1981; Masters and Gilbert, 1983; Widmer et al., 1991; Durek and Ekström, 1996)). In other words, they assume that, within the seismic band,  $\alpha$  cannot be resolved and thus implicitly rely on the frequency-independent attenuation model of Kanamori and Anderson (1977). Anderson and Given (1982) created the only model of both the frequency and depth dependence of attenuation by relating them through a physical model of the underlying relaxation mechanisms. The exact nature of mantle relaxation processes is, however, still debated (e.g. Jackson and Anderson, 1970; Karato and Spetzler, 1990). In this paper, we develop and apply a new method based on the standard analysis of Backus and Gilbert (1970) that allows us to separate the effects of the radial  $q$  profile from those due to frequency dependence of  $q$  as described by  $\alpha$ . Therefore, we are able to eliminate the tradeoffs present in previous studies and to focus on determining  $\alpha$  without having to construct a new radial  $q$  profile or a full absorption band model of attenuation in the mantle. Our method also makes it possible to move beyond the assumption of frequency-independent attenuation without relying on model-dependent physical constraints, as (Anderson and Given, 1982) had done. In what follows, we carry out a suite of synthetic tests which explore the characteristics of the available attenuation measurements. We also attempt to extract  $\alpha$  from available long-period seismic attenuation data.

## 2. Method

We here modify the standard analysis of the resolution provided by a set of measurements (Backus and Gilbert, 1970), which has been recently applied to the study of radial density resolution within the Earth (Masters and Gubbins, 2003). Our goal is to adapt this analysis in order to extract the signal of frequency dependence of seismic attenuation.

We can relate a mode attenuation measurement  $q$  to material properties within the Earth via sensitivity (Fréchet) kernels  $K_\mu$  and  $K_\kappa$  (e.g. Dahlen and Tromp, 1998):

$$q = \int_0^R dr (\kappa_0 q_\kappa K_\kappa + \mu_0 q_\mu K_\mu), \quad (1)$$

where  $R$  is the radius of the Earth,  $\kappa_0$  and  $\mu_0$  are the reference radial profiles of bulk and shear moduli, and  $q_\kappa$  and  $q_\mu$  are values of radial bulk and shear attenuation. In this study we use either PREM (Dziewonski and Anderson, 1981) or ak135 (Kennett et al., 1995) as the elastic, and QL6 (Durek and Ekström, 1996) or QM1 (Widmer et al., 1991) as the attenuation reference profiles. We calculate the relevant frequencies of oscillation and sensitivity kernels  $K_\mu$  and  $K_\kappa$  using a modified MINOS (Woodhouse, 1998) code (Capdeville, personal communication). The results of our analysis are valid insofar as the deviations of  $q$  from the reference profile remain sufficiently small to not affect the kernels themselves.

All the quantities in the integrand of Eq. (1) are functions of radius. We proceed to discretize them with respect to radius, so that they can be written in vector form, e.g.  $K_\mu(r)$  becomes  $\mathbf{K}_\mu$ . For the frequency range considered in this study, we verify that the discretization is sufficiently dense.

It is important to observe that the sensitivity kernels of fundamental modes with similar frequencies are very similar. Therefore, existing  $q$  datasets are likely to be highly redundant (Masters and Gilbert, 1983). We seek to exploit this redundancy and divide modes into a low and high-frequency bin, denoted by superscript  $l$  and  $h$ , respectively. Each linear combination of Fréchet kernels of modes in each bin defines a new “hyperkernel”:

$$\mathbf{H}_{\mu,\kappa}^{\text{low}} = \sum_{l=1}^{N_l} \gamma^l \mathbf{K}_{\mu,\kappa}^l \quad \text{and} \quad \mathbf{H}_{\mu,\kappa}^{\text{high}} = \sum_{h=1}^{N_h} \gamma^h \mathbf{K}_{\mu,\kappa}^h, \quad (2)$$

where  $N_l$  and  $N_h$  are the number of modes in each bin, and the subscripts  $\mu$  and  $\kappa$  denote that the kernels refer to either shear or bulk attenuation. Though called averaging kernels by Backus and Gilbert (1970), we have dubbed them “hyperkernels” to stress their usefulness for separating the effects of the depth dependence of attenuation from its frequency dependence.

Each particular choice of  $\gamma^l$  and  $\gamma^h$  will yield hyperkernels with different depth sensitivities. Therefore, by requiring that  $\gamma^l$  and  $\gamma^h$  yield hyperkernels with identical sensitivities to the radial attenuation profile, it is possible to remove the tradeoff between depth- and frequency dependence of attenuation measurements. Since we focus on the effective  $\alpha$  in the mantle, we also seek to eliminate the contamination from the inner core while averaging mantle structure. We do this by requiring the hyperkernels to be zero in the core while providing maximally uniform sensitivity in the mantle. In order to eliminate the contribution from poorly-constrained mantle bulk attenuation, we seek hyperkernels that are insensitive to  $q_\kappa$ . These three coupled constraints can be written as:

$$\mathbf{H}_\mu^{\text{high}} = \mathbf{H}_\mu^{\text{low}} \quad \text{and} \quad \mathbf{H}_\mu^{\text{high}} = \mathbf{H}_\mu^{\text{low}} = \mathbf{b} \quad \text{and} \quad \mathbf{H}_\kappa^{\text{low}} = \mathbf{H}_\kappa^{\text{high}} = \mathbf{0} \quad (3)$$

where  $\mathbf{b}$  is unity in the mantle and zero elsewhere. While the first constraint is paramount, the others cannot be satisfied exactly and require the introduction of a damping parameter,  $\lambda_1$ . In light of Eq. (2), we write these conditions in condensed matrix notation as  $\mathbf{P} \cdot \boldsymbol{\Gamma} = \mathbf{B}$  or as:

$$\begin{pmatrix} \mathbf{K}_\mu^l & -\mathbf{K}_\mu^h \\ \lambda_1 \mathbf{K}_\mu^l & \mathbf{0} \\ \mathbf{0} & \lambda_1 \mathbf{K}_\mu^h \\ \mathbf{K}_\kappa^l & \mathbf{0} \\ \mathbf{0} & \mathbf{K}_\kappa^h \end{pmatrix} \begin{pmatrix} \gamma^l \\ \gamma^h \end{pmatrix} = \begin{pmatrix} \mathbf{0} \\ \lambda_1 \mathbf{b} \\ \lambda_1 \mathbf{b} \\ \mathbf{0} \\ \mathbf{0} \end{pmatrix}. \quad (4)$$

The damping parameter  $\lambda_1$  allows us to select among all combinations of nearly-identical hyperkernels those that have zero sensitivity to  $q_\kappa$  and inner core  $q_\mu$ . Ideally, our hyperkernels would only use modes whose attenuation measurements have the smallest published uncertainties. Therefore, we seek  $\gamma^l$  and  $\gamma^h$  that minimize the squared misfit:

$$S = \mathbf{B} - \mathbf{P} \cdot \boldsymbol{\Gamma} + \lambda_2 \mathbf{V} \cdot \mathbf{I}, \quad (5)$$

where  $\mathbf{V}$  is a vector containing published variances of the  $q$  measurements of individual modes in both bins,  $[\nu^l, \nu^h]$ , and  $\lambda_2$  is a constant that sets the importance of the constraint on minimizing the resulting uncertainties.

To each hyperkernel corresponds a  $q$  value, which is a weighted average of the  $q$  measurements of its constituent normal modes:

$$q^{\text{low}} = \sum_{l=1}^{N_l} \gamma^l q^l \quad \text{and} \quad q^{\text{high}} = \sum_{h=1}^{N_h} \gamma^h q^h. \quad (6)$$

Furthermore, if we assume that the uncertainties in the attenuation measurements of the low and high-frequency modes are uncorrelated, we can directly relate variances  $\nu$  ( $\nu \equiv \sigma^2$ ) in the mode  $q$  measurements to uncertainties in  $q^{\text{low}}$  and  $q^{\text{high}}$  via

$$\nu^{\text{low}} = \sum_{l=1}^{N_l} \gamma^l \nu^l \gamma^l \quad \text{and} \quad \nu^{\text{high}} = \sum_{h=1}^{N_h} \gamma^h \nu^h \gamma^h. \quad (7)$$

Since the two hyperkernels have identical sensitivity to radial attenuation structure but differing frequency content, differences in  $q^{\text{low}}$  and  $q^{\text{high}}$  can be attributed to frequency dependence of

**Table 1**  
The four choices of upper and lower bounds on low and high-frequency bins used in this study.

	Low-frequency bin			High-frequency bin		
	Upper bound	Lower bound	Number of modes	Upper bound	Lower bound	Number of modes
	(s)	(s)		(s)	(s)	
A	3231	600	35	600	10	168
B	3231	700	26	700	500	23
C	700	500	23	400	200	70
D	400	200	70	200	10	58

For each bin, the number of modes with available measurements is also listed.

attenuation. These effects of frequency dependence can be accounted for by projecting the individual mode  $q$ 's to a reference value  $q_0$  using:

$$q_{0i} = q_i \left( \frac{\omega_i}{\omega_0} \right)^\alpha \quad (8)$$

In the absence of systematic measurement error,  $q^{\text{low}}$  and  $q^{\text{high}}$  will be reconciled at the reference frequency for the value of  $\alpha$  that corresponds to the effective  $\alpha$  of the mantle. Note that this correction for the effects of frequency dependence must also be applied to variances  $\mathbf{V}$ , and therefore affects the misfit function and through it the retrieved coefficients,  $\gamma$ .

For each test value of  $\alpha$  we can use the uncertainty on the  $q$  measurement of the hyperkernels (i.e.  $\nu^{\text{low}}$  and  $\nu^{\text{high}}$ ) to calculate the probability that the  $q^{\text{low}}$  and  $q^{\text{high}}$  can be considered identical at the reference frequency. Since the  $q$  of each hyperkernel can be represented by two Gaussian probability density functions (PDFs) with means  $q^{\text{low}}$  and  $q^{\text{high}}$  and variances  $\nu^{\text{low}}$  and  $\nu^{\text{high}}$ , we seek to calculate the likelihood that sample  $q$  values drawn at random from these two PDFs can be considered identical. The PDF that describes the difference between the two random samples is described by a Gaussian of mean  $q^{\text{low}} - q^{\text{high}}$  and variance  $\nu^{\text{low}} + \nu^{\text{high}}$ . In addition to measurement uncertainty, the damping contributes to the uncertainties of  $q^{\text{low}}$  and  $q^{\text{high}}$  by preventing the two hyperkernels from being identical. We restrict this uncertainty to be small by requiring that the attenuation values predicted by the two hyperkernels for an identical radial attenuation profile are within 3% of one another. This is why we consider  $q^{\text{low}}$  and  $q^{\text{high}}$  to be reconciled by a test value of  $\alpha$  if their difference is less than 3%. The value of 3% was found to be the most stringent value that could be satisfied for a large range of damping parameters.

Having calculated the probability that a trial  $\alpha$  value reconciles  $q^{\text{low}}$  and  $q^{\text{high}}$ , we can proceed to conduct a search for an optimal value of  $\alpha$  which would maximize this probability. For the particular choice of damping parameters  $\lambda_1$ , and  $\lambda_2$  used in constructing the hyperkernels, this optimal  $\alpha$  value is taken to be the measurement of effective mantle  $\alpha$ .

### 3. Results

#### 3.1. Method validation

Armed with a method which has the potential to separate the depth- and frequency dependence of attenuation, we first proceed to quantify its  $\alpha$ -resolving power. At the same time, we investigate whether the existing normal mode attenuation measurements are sufficiently numerous and precise for constraining  $\alpha$ . To this end, we perform a series of synthetic tests in which we generate  $q$  values of modes whose attenuation has been measured. We assume the radial attenuation profile QL6 together with PREM elastic structure, because the QL6 model fits the Earth-orbiting surface waves better than the attenuation structure of PREM. We adopt a depth-invariant  $\alpha$  value of 0.3 throughout the mantle and assume frequency-independent

attenuation, i.e.  $\alpha=0$ , in the inner core. To each synthetic mode  $q$  we assign the same variance  $\nu$  as that of the corresponding real measurement. Generated  $q$ 's and the corresponding kernels  $K_{\mu\kappa}$  are then distributed within two distinct frequency bins. There are, of course, multiple choices for the frequency content of each bin. Table 1 specifies the frequency content and number of modes with available measurements for the four different binning schemes used in this study.

In order to find the most likely  $\alpha$  value, we explore  $\alpha$  values between  $-1$  and  $+1$  subject to a range of damping parameters  $\lambda_1$  and  $\lambda_2$  from  $10^{-4}$  to  $1$  and from  $10^{-6}$  to  $10^{-2}$ , respectively. The values of  $\lambda_1$  and  $\lambda_2$  have to be small in order to ensure that the hyperkernels have identical shape. Fig. 2 (top row) shows the retrieved effective  $\alpha$  for the four different binning schemes (labeled from A to D), with warm colors indicating higher probabilities than the cool colors. For all binning choices, the greatest likelihood is in excellent agreement with the initial value of  $\alpha$  regardless of the value assigned to the damping parameter  $\lambda_2$ , which controls the resulting variance. We stress that the retrieved likelihoods are stable over a large range of damping parameters  $\lambda_1$  and  $\lambda_2$ . Based on Fig. 2, we conclude that the number and precision of existing attenuation measurements are indeed sufficient to retrieve accurately the frequency dependence of attenuation.

As expected, the uncertainty on the  $\alpha$  measurement decreases as the variance damping  $\lambda_2$  increases. But, values of  $\lambda_2$  that are too large can result in significant differences between hyperkernels and contaminate the extracted value of  $\alpha$ . Note that in the case of the choice D (high-frequency bins), the uncertainty of the retrieved  $\alpha$  is considerably larger than in the case when lower frequency modes are included. This is because the higher frequency overtone attenuation measurements are generally less precise than the measurements made at lower frequencies. The blanked areas correspond to situations when the difference in the hyperkernels exceeded 3%.

The hyperkernels  $\mathbf{H}_\mu^{\text{low}}$  and  $\mathbf{H}_\mu^{\text{high}}$  corresponding to schemes A–D are plotted in Fig. 2 (bottom row). The hyperkernels are almost indistinguishable (the difference is less than 3%) and they vanish in the core. As for the hyperkernels  $\mathbf{H}_\kappa^{\text{low}}$  and  $\mathbf{H}_\kappa^{\text{high}}$ , they remain negligible throughout the whole Earth. Peak of the sensitivity with depth reflects the frequency content of the corresponding binning schemes; while lower frequency modes sample the entire mantle (A and B), the higher frequency ones only sample shallower regions (C and D).

We have also tested other binning schemes (not listed in Table 1) and other values of input  $\alpha$ , and our method consistently retrieves the correct  $\alpha$  value. Changing the bounds of the frequency bins results in a different population of modes in each bin. As a result, the optimized hyperkernels may change as may the uncertainties on the  $\alpha$  measurement. When the frequency contents of the two hyperkernels are made to be very different, the problem of finding a linear combination of mode sensitivities that will satisfy the three constraints of Eq. (3) becomes more difficult. At the same time, hyperkernels with frequency content that is too similar have difficulty resolving the effects of frequency dependence of attenuation, as observed in panel D of Fig. 2.



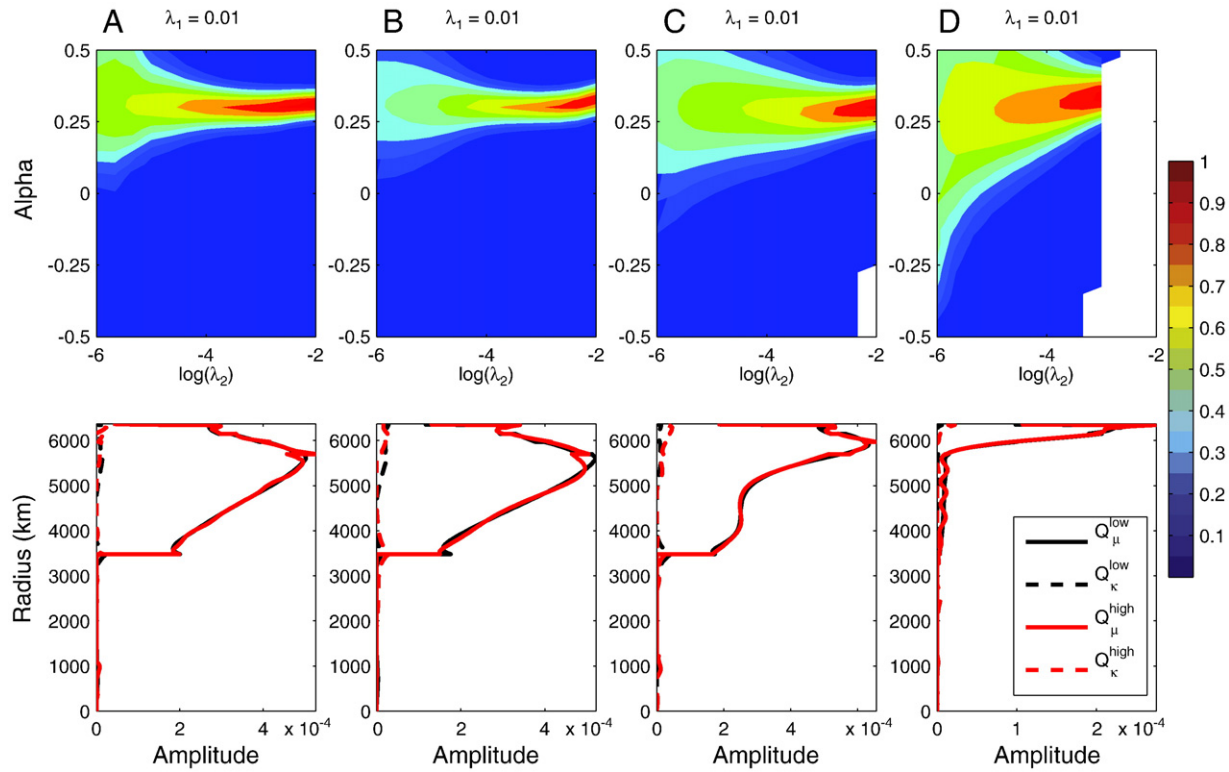


**Fig. 2.** Top row: The retrieved  $\alpha$  likelihoods for a synthetic dataset with input  $\alpha = 0.3$  for the four different binning schemes (A, B, C, D) detailed in Table 1. Warm colors indicate greater likelihoods than cool colors. The retrieved  $\alpha$  is in excellent agreement with the input value, and it is independent of  $\lambda_2$ . Bottom row: The hyperkernels associated with the four binning schemes for  $\lambda_1 = 0.01$  and  $\lambda_2 = 4.10^{-4}$ .  $H_\kappa^{\text{low,high}}$  are nearly zero everywhere in the Earth, and  $H_\mu^{\text{low,high}}$  have no sensitivity to inner core structure and nearly-identical sensitivity in the mantle.

### 3.2. Effective $\alpha$ in the mantle

Having validated our approach, we apply our methods to the real  $q$  measurements. We use a compilation of original measurements and published data provided by (Masters, personal communication). Fig. 3 (top row) shows the retrieved  $\alpha$  likelihoods for the same binning schemes listed in Table 1. The retrieved  $\alpha$  likelihoods are characterized by strikingly different trends than those extracted from our synthetic tests that assumed a frequency- and depth-independent  $\alpha$ . When all available measurements are used (binning scheme A), the most prominent characteristic is a systematic increase of retrieved  $\alpha$  with increasing  $\lambda_2$ . Highest likelihoods are reached at a zero value of effective  $\alpha$  in the mantle. Analysis of the lowest-frequency measurements (binning scheme B) accentuates this trend, while indicating a negative value of effective  $\alpha$ . When modes of intermediate frequency are used (binning scheme C), the character of the retrieved  $\alpha$  likelihoods changes significantly. The most likely effective  $\alpha$  in this frequency range is 0.1, and is largely independent of the value of  $\lambda_2$ . Moving onward to the highest available frequencies (binning scheme D), the most likely  $\alpha$  values are positive, lingering around a value of 0.3, but suffering from large uncertainties.

These systematic changes in behavior of retrieved  $\alpha$  are clearly incompatible with a constant  $\alpha$  model, regardless of its absolute value. Therefore, neither the usual assumption of frequency-independent attenuation often used in seismology (e.g. Dziewonski and Anderson, 1981; Kanamori and Anderson, 1977), nor the constant non-zero  $\alpha$  models suggested by laboratory studies (Jackson et al., 2002), allow us to explain the observations. In fact, Fig. 3 strongly suggests that  $\alpha$  varies with frequency within the absorption band. In particular, mantle  $\alpha$  appears to be negative at periods longer than 1000 s, transitioning to a small positive value in the period range  $\sim 1000$ –700 s, and increasing again at periods shorter than 500 s. It is important to realize that noise in the attenuation measurements

might introduce artifacts in the retrieved  $\alpha$  signal. However, the observed systematic behavior is likely to be a robust feature.

#### 3.2.1. Frequency dependence of $\alpha$

In order to better constrain the variation of effective  $\alpha$  with frequency, we perform a series of forward-modeling exercises. We start by allowing a single jump in  $\alpha$  from negative to positive values, i.e. we assume that at long periods  $q$  increases with increasing frequency, while at short periods,  $q$  decreases with increasing frequency. We create several dozen trial models by varying the frequency position and magnitude of the jump. Each of these models is used to calculate a synthetic dataset, which is then analyzed in the same way as the actual measurements. We find that no model with a single jump in  $\alpha$  is capable of capturing the complex character of the retrieved  $\alpha$  shown in the top row of Fig. 3. Nevertheless, models in which  $\alpha$  transitions from negative to positive in the  $\sim 1000$ –400 s period range reproduce the character observed in the data better than any constant  $\alpha$  model.

Allowing for a more complex frequency-dependent character of  $\alpha$ , we fashion a set of trial models characterized by jumps in  $\alpha$  at two different frequencies. Given uncertainties in the attenuation measurements and the possibly complex behavior of mantle  $\alpha$ , no single model is likely to explain all the features present in Fig. 3 (top row). However, we find that a model in which  $\alpha$  changes from a value of  $-0.4$  at periods longer than 1000 s, to a value of 0.1 in the period range 300–800 s, before changing to 0.3 at periods shorter than 200 s, reproduces well the overall features present in the data (see bottom row of Fig. 3). Our preferred model is shown in Fig. 4 and it is compared with laboratory studies and the frequency-independent assumption. Since our study did not constrain the value of  $q^{-1}$ , we have assumed that the high-frequency corner occurs at 1 Hz where  $q^{-1}$  is 600 (Sipkin and Jordan, 1979) in constructing the figure. Of course, our preferred model of  $\alpha$  should be viewed as an example of a set of possible models, which must share its

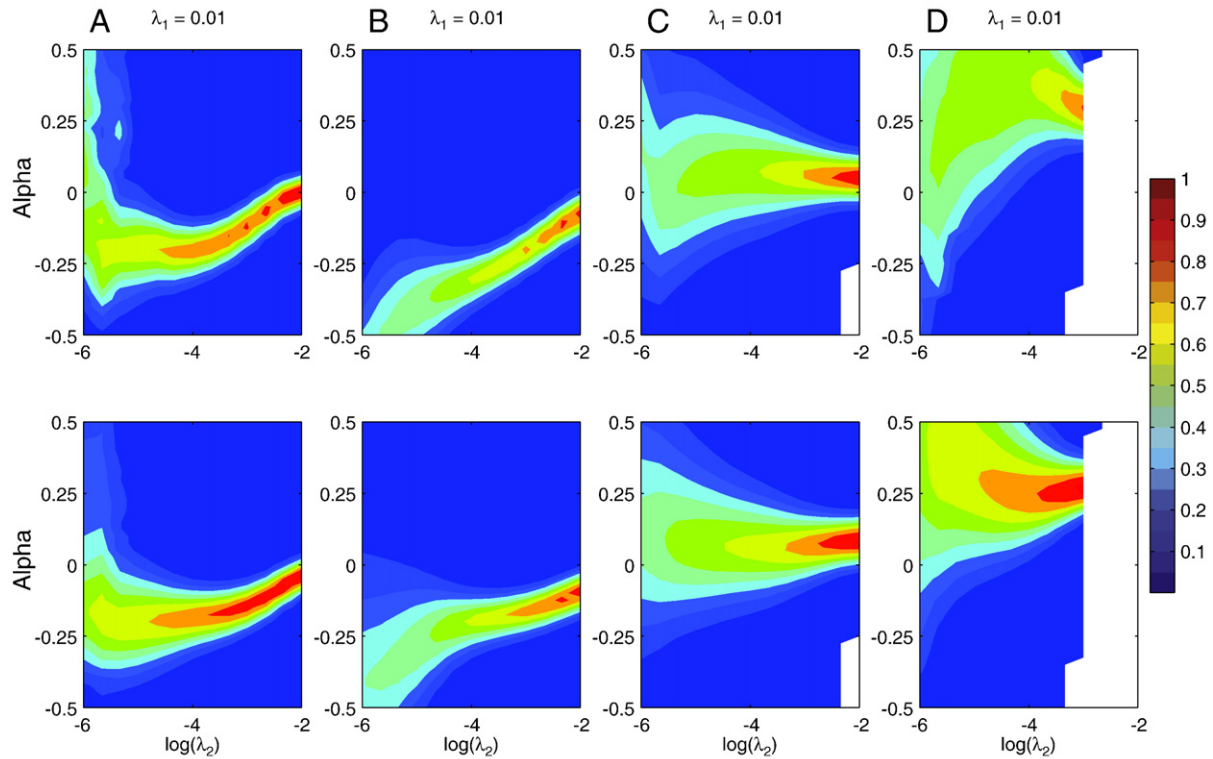


**Fig. 3.** Top row: The retrieved  $\alpha$  likelihoods for actual attenuation measurements binned according to the four different schemes (A, B, C, D) listed in Table 1. Warm colors indicate greater likelihoods than do cool colors. Bottom row: Similar overall behavior is obtained from synthetic  $q$  values generated using our preferred model of frequency-dependent  $q$  (see text).

distinguishing features: a negative  $\alpha$  at periods longer than 1000 s, and a positive and increasing  $\alpha$  at shorter periods.

### 3.2.2. Depth dependence of $\alpha$

In order to investigate possible depth dependence of  $\alpha$ , we have fashioned hundreds of models in which we allow  $\alpha$  to vary with both frequency and depth. In these models,  $\alpha = -1$  at periods longer than

a prescribed critical period  $T_c$ , whereas it is allowed to take on values between 0.0 and 0.3 at periods shorter than  $T_c$ . We then allow  $T_c$  to vary between 1000 s and 400 s in three different regions of the mantle: the upper mantle, transition zone, and lower mantle. None of the explored models fits the data as well as the preferred model shown in Fig. 4; they are particularly inadequate in capturing the character of the high-frequency data seen in panel D of Fig. 3.

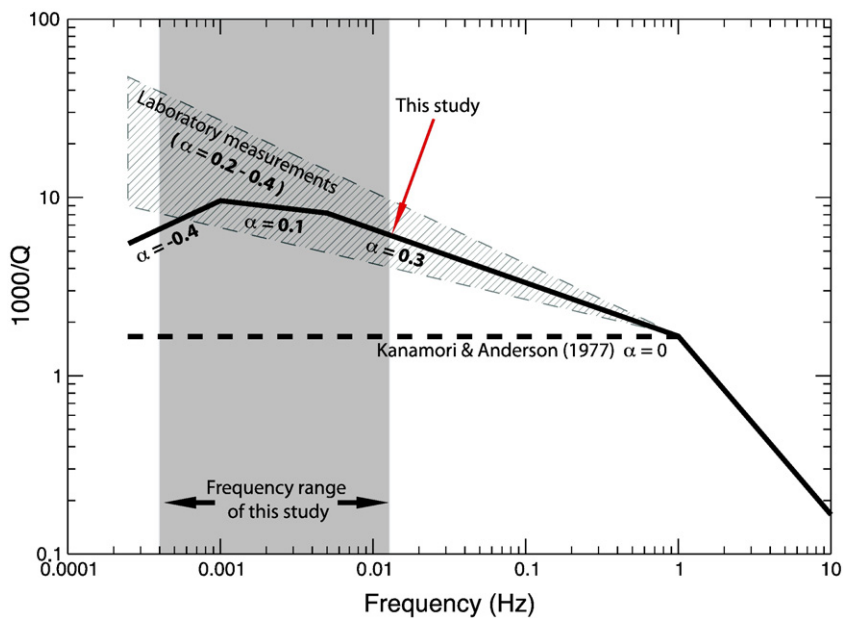


**Fig. 4.** Preferred model (solid line) of frequency dependence of attenuation within the absorption band compared with constraints from laboratory studies (hatched region) and the frequency-independent assumption (dashed line). In our model,  $\alpha$  is approximately 0.3 at periods shorter than 200 s, decreasing to 0.1 in the period range 300–800 s, and becoming negative ( $-0.4$ ) at periods longer than 1000 s. We assume that the high-frequency corner occurs at 1 Hz where  $q^{-1}$  is 600, past which frequency  $\alpha$  is 1 (Sipkin and Jordan, 1979). It is important to emphasize that we constrain the value of  $\alpha$  and not of  $q^{-1}$ .

Nevertheless, the subset of the explored models that is capable of explaining the low-frequency features (panels A, B and C of Fig. 3) has  $T_c = 1000$  s and  $\alpha = 0.1$  at periods shorter than  $T_c$  at all depths.

Because of the shape of the hyperkernels used in this study, our method is only weakly sensitive to  $\alpha$  and  $T_c$  values in thin layers, such as the transition zone and  $D''$ . Indeed, because forward-modeling tests indicated that our sensitivity to the  $D''$  region was nearly negligible, we have not parameterized it as distinct from the lower mantle. This lack of sensitivity implies that even though none of the models in which  $T_c$  or  $\alpha$  varied significantly with depth were able to reproduce the behavior observed in Fig. 3, we cannot rule out smaller variations in  $T_c$ , or even significant variations within thin layers such as  $D''$ .

For completeness, one might consider models in which the value of  $\alpha$  is the same below and above  $T_c$ , which corresponds to a model in which  $\alpha$  varies with depth but not frequency. However, this class of models has not been considered as a plausible solution to explain the available attenuation measurements. Such a frequency-independent model would require negative  $\alpha$  values across a wide range of frequencies in large sections of the mantle in order to match the characteristics observed in the top row of Fig. 3. Such behavior has been suggested by neither theoretical studies nor by experiments, and is thus highly unlikely.

We note that these results are robust across different reference Earth models. The character of the retrieved  $\alpha$  likelihoods remains largely unchanged when ak135 (Kennett et al., 1995) is used instead of PREM (Dziewonski and Anderson, 1981). Using the QM1 (Widmer et al., 1991) radial profile of attenuation instead of QL6 (Durek and Ekström, 1996) similarly only marginally affects the retrieved likelihoods, confirming the fact that our method allows us to constrain  $\alpha$  independently of the radial attenuation profile. Of course, using inappropriate reference models can result in sensitivity kernels sufficiently different from those corresponding to the actual measurements to obliterate the sought-after  $\alpha$  signal.

#### 4. Discussion

We have devised a method capable of separating the frequency dependence of attenuation from its depth dependence. After validating our method on a synthetic dataset, we demonstrated that the number and precision of existing attenuation measurements are sufficient for constraining  $\alpha$ . Applying the approach to actual attenuation measurements of free oscillations and surface waves spanning the period range 3200 s–50 s, we observed that effective  $\alpha$  is likely to be frequency dependent. Specifically,  $\alpha$  is negative at periods longer than 1000 s and positive and increasing from approximately 0.1 to 0.3 at shorter periods (see Fig. 4). This conclusion runs against both the assumption of frequency-independent attenuation often used in seismology, and the constant, positive  $\alpha$  model suggested by laboratory studies (Jackson et al., 2005).

Having constrained  $\alpha$  and its frequency dependence, we explored a large set of models in which  $\alpha$  varied with both frequency and depth. Our tests were motivated by the expectation that  $\alpha$  in the Earth depends on both frequency and depth, since the pressure- and temperature dependence of the activation enthalpy of the relaxation mechanisms giving rise to the absorption band may induce a shift in its frequency extent with depth (Jackson and Anderson, 1970; Anderson and Minster, 1979; Minster and Anderson, 1981; Anderson and Given, 1982). Despite this expectation, we were unable to observe any significant variation of  $\alpha$  with depth.

Our frequency-dependent model of  $\alpha$  is physically plausible, and was suggested by the pioneering study of Anderson and Given (1982) who constructed a mantle attenuation model (ABM) in which the frequency location of the absorption band changed with depth. While the ABM predicted positive  $\alpha$  values in the midmantle for all frequencies considered in our study, their upper and lowermost mantle regions were characterized by negative  $\alpha$  values at periods longer than 1000 s. This is consistent with our findings. Further direct comparisons between

our preferred model and the ABM are not straightforward, since Anderson and Given (1982) modeled both the depth- and frequency dependence of attenuation, whereas the novelty of our approach rests in its ability to constrain the frequency dependence of attenuation independently of its radial profile. We have also re-analyzed the dataset used by Anderson and Given (1982) using our method, and found that the number and quality of the measurements available to them were insufficient for a reliable estimation of  $\alpha$ . Indeed, Anderson and Given (1982) noted the lack of resolution of  $\alpha$  and used only modes sensitive to the midmantle in order to constrain its value at 0.15. Both our novel approach and the dramatic improvement in the precision and number of available attenuation measurements – we use twice as many as were available a quarter-century ago – has made it possible to constrain the complex character of  $\alpha$  in the mantle in a way that was unavailable when ABM was created.

In addition to being physically plausible, our preferred model of frequency dependence of attenuation is consistent with earlier studies that have relied upon body waves and have focused on higher frequencies (see Fig. 4). A number of studies (Ulug and Berckhemer, 1984; Cheng and Kennett, 2002) looking at S/P ratios at frequencies greater than 40 mHz have argued for  $\alpha$  values in the 0.1–0.6 range. Shito et al. (2004) used continuous P-wave spectra to constrain  $\alpha$  between 0.2 and 0.4 at periods shorter than 12 s, while Flanagan and Wiens (1998) found that an  $\alpha$  value of 0.1–0.3 was needed to reconcile attenuation measurements on sS/S and pP/P phase pairs in the Lau basin. Unlike these studies, however, our model of  $\alpha$  relies upon data that provide more uniform global coverage, and, therefore, ought to more closely approximate the  $\alpha$  representative of the average mantle.

A non-zero value of  $\alpha$  carries important implications for the construction of radial profiles of attenuation. Efforts at determining the radial profile of attenuation in the Earth have routinely assumed that attenuation is frequency independent (e.g. Dziewonski and Anderson, 1981; Durek and Ekström, 1996). The resulting models have, therefore, mapped the signal of frequency dependence of  $q$  into its depth profile. The extent to which neglecting the frequency dependence of  $\alpha$  contaminates the true depth profiles of  $q$  can be probed by comparing the magnitude of the variation in measured values of  $q$  to the variation expected for different values of  $\alpha$ . Such a comparison is attempted in Fig. 5, which shows the effects that  $\alpha$  can

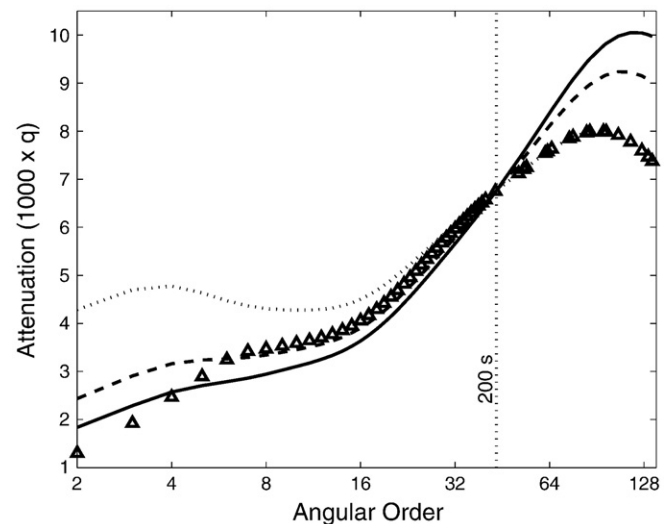


Fig. 5. The effect of  $\alpha$  on attenuation measurements can be significant. The solid line represents the attenuation values predicted by QL6. If we consider these predictions as representative of the  $q$  structure at a period of 200 s, then values of  $\alpha$  of 0.1 and 0.3 would result in  $q$  values indicated by the dashed and dotted lines, respectively. The effect obtained in the same fashion but using our preferred model of  $\alpha$  is delineated by triangles. Note that the signal of frequency dependence of attenuation can be significantly larger than the discrepancies between the normal mode and surface wave measurements shown in Fig. 1.



have on attenuation measurements; for our preferred model, the effects of  $\alpha$  on attenuation can be very significant. Therefore, we expect that the existing radial profiles of attenuation are likely to be contaminated, and that they should not be used as-is to constrain the thermochemical state of the Earth's interior. Nevertheless, if these models are to be used solely for modeling the effects of Earth structure on seismic waves, then mapping the frequency dependence of attenuation into its radial profile is not a problem.

The dependence of intrinsic attenuation on temperature can be described by the following expression (e.g. Romanowicz and Mitchell, 2007):

$$q \propto \omega^{-\alpha} \exp(-\alpha H / RT) \tag{9}$$

where  $H$  is the activation enthalpy,  $R$  is the gas constant, and  $T$  is the temperature. The value of  $\alpha$ , then, determines the functional form of  $\partial q / \partial T$ . When  $\alpha$  is zero,  $\partial q / \partial T$  is independent of temperature, whereas when  $\alpha$  is positive,  $\partial q / \partial T$  is exponentially dependent on temperature (Minster and Anderson, 1981). Recent studies seeking to constrain lateral attenuation variations rely on data with periods shorter than ~300 s (e.g. Gung and Romanowicz, 2004). At these periods, our preferred model suggests a positive  $\alpha$  value close to 0.3. This value implies an exponential temperature dependence of attenuation, and justifies the interpretation of lateral attenuation variations in terms of temperature variations. Note that the amplitude of lateral temperature variations necessary to obtain the observed  $q$  signal are therefore smaller than would be in the case of frequency-independent attenuation. Similarly, a positive  $\alpha$  value affects the anelastic correction to the velocity-temperature relationships that need to be used when interpreting the lateral seismic velocity variations (Romanowicz, 1994; Matas and Bukowski, 2007).

Intrinsic attenuation causes dispersion of seismic velocities, decreasing the velocities of longer period waves compared to shorter period ones. Properly correcting for the dispersion effect is crucial when datasets with different frequency content are used to simultaneously constrain velocities in the Earth (Kanamori and Anderson, 1977). Usually, the difference in wave-speeds due to an attenuation value  $q$  at two frequencies  $\omega_{1,2}$  is calculated using the expression

$$\frac{V(\omega_2)}{V(\omega_1)} = 1 + \frac{q}{\pi} \ln\left(\frac{\omega_2}{\omega_1}\right), \tag{10}$$

which is only valid when  $\alpha=0$ . However, non-zero values of  $\alpha$ , as suggested by this study, require the use of a different dispersion correction (Anderson and Minster, 1979; Minster and Anderson, 1981)

$$\frac{V(\omega_2)}{V(\omega_1)} = 1 + \frac{q(\omega_1)}{2} \cot\left(\frac{\alpha\pi}{2}\right) \left[1 - \left(\frac{\omega_1}{\omega_2}\right)^\alpha\right]. \tag{11}$$

We can see from this expression that the values of  $\alpha$  and  $q(\omega_1)$  will significantly affect the magnitude of the dispersion correction. The relative difference between these two expressions, though, is independent of  $q$ . For an  $\alpha$  value of 0.3, the assumption of frequency-independent attenuation will result in 25% error for a frequency ratio of 10 and a 50% error for a frequency ratio of 100. Assuming that  $\alpha=0$  substantially overestimates the velocity dispersion, as pointed out by Anderson and Minster (1979) and results in differences that are not negligible when compared to those between different models of Earth's 1D velocity structure (see Fig. 6). Indeed, the effect of non-zero  $\alpha$  can be larger than the correction applied to seismic velocities measured at high frequencies using spectroscopic laboratory methods. We note that Eq. (10) is valid for frequency-independent  $\alpha$ . When  $\alpha$  varies within the frequency range over which the dispersion correction is applied (i.e.  $\omega_1$  to  $\omega_2$ ), Eq. (10) should be applied separately to each domain of constant  $\alpha$ .

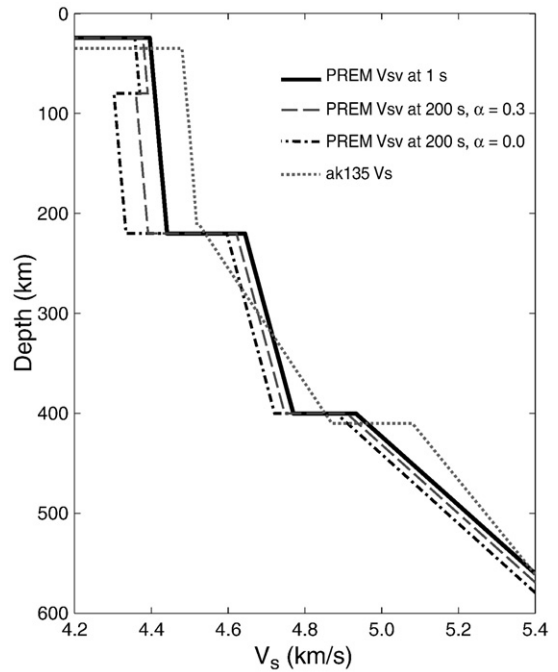


Fig. 6. Accounting for the effects of frequency dependence of attenuation is crucial for velocity dispersion corrections. The solid line represents the  $V_{sv}$  profile of PREM in the top 600 km of the mantle at the reference period of 1 s. By taking the PREM shear attenuation structure to be appropriate at 200 s (since it is derived from normal mode attenuation measurements) and a value of  $\alpha$ , we can account for velocity dispersion due to attenuation. We calculate  $V_{sv}$  at a reference period of 200 s using  $\alpha=0$  (dash-dotted line) and  $\alpha=0.3$  (long-dashed line). Assuming that  $\alpha=0$  substantially overestimates the velocity dispersion, as pointed out by Anderson and Minster (1979). The difference between the profiles with different  $\alpha$  values are similar in magnitude to those between different models of Earth's 1D velocity structure, such as ak135 (dotted line) and PREM.

Finally, the precise knowledge of seismic velocity, its dispersion and associated attenuation is important for meaningful comparisons with other geophysical observables, such as the geoid (e.g. Romanowicz, 1990). For example, estimations of viscosity of the lower mantle are based on values of  $R_{s/\rho} = \partial \ln V_s / \partial \ln \rho$  parameter that (e.g. Richards and Hager, 1984; Ricard et al., 1993) do not include the anelastic effects. Matas and Bukowski (2007) showed that anelasticity may significantly affect the value of  $R_{s/\rho}$  and  $R_{p/\rho}$ , but pointed out that a more precise knowledge of the absorption band and its characteristics is still needed. Future work should thus be aimed at improving the precision of  $q$  measurements and the development of radial  $q$  profiles that properly account for the frequency dependence of  $q$ .

**Acknowledgments**

This project was supported by the National Science Foundation (through NSF grants EAR-0336951 and EAR-0738284) and by French CNRS-SEDIT program during the stay of JM at University of California, Berkeley. VL acknowledges support through a Graduate Research Fellowship from the National Science Foundation. We wish to thank Guy Masters for kindly providing us his attenuation measurement compilation and, along with Mark S.T. Bukowski, for inspiring discussions that helped improve the manuscript. This is Berkeley Seismological Laboratory contribution no. 09-05.

**References**

Anderson, D., 1976. The Earth as a seismic absorption band. *Science* 196, 1104–1106.  
 Anderson, D., Given, J., 1982. Absorption band Q model for the Earth. *J. Geophys. Res.* 87, 3893–3904.  
 Anderson, D., Hart, R., 1978. Q of the Earth. *J. Geophys. Res.* 83, 5869–5882.



- Anderson, D., Minster, J., 1979. The frequency dependence of  $Q$  in the Earth and implications for mantle rheology and Chandler wobble. *Geophys. J. R. Astron. Soc.* 58, 431–440.
- Backus, G.E., Gilbert, J.F., 1970. Uniqueness in the inversion of inaccurate gross Earth data. *Philos. Trans. R. Soc. Lond.* 266, 123–192.
- Cheng, H.X., Kennett, B., 2002. Frequency dependence of seismic wave attenuation in the upper mantle beneath the Australian region. *Geophys. J. Int.* 150, 45–57.
- Dahlen, F., Tromp, J., 1998. *Theoretical Global Seismology*. University Press, Princeton.
- Dalton, C.A., Ekström, G., 2006. Global models of surface wave attenuation. *J. Geophys. Res.* 111 (B10), 5317.
- Durek, J., Ekström, G., 1996. A radial model of anelasticity consistent with long-period surface-wave attenuation. *Bull. Seismol. Soc. Am.* 86, 155–158.
- Durek, J.J., Ekström, G., 1997. Investigating discrepancies among measurements of traveling and standing wave attenuation. *J. Geophys. Res.* 102, 24529–24544.
- Dziewonski, A.M., Anderson, D.L., 1981. Preliminary reference Earth model. *Phys. Earth Planet. Inter.* 25, 297–356.
- Flanagan, M.P., Wiens, D.A., 1998. Attenuation of broadband P and S waves in Tonga: observations of frequency dependent  $Q$ . *Pure Appl. Geophys.* 153, 345–375.
- Gung, Y., Romanowicz, B., 2004.  $Q$  tomography of the upper mantle using three-component long-period waveforms. *Geophys. J. Int.* 157, 813–830.
- Jackson, D., Anderson, D., 1970. Physical mechanisms of seismic-wave attenuation. *Rev. Geophys.* 8, 1–63.
- Jackson, I., Fitz-Gerald, J., Faul, U., Tan, B., 2002. Grain-size-sensitive seismic wave attenuation in polycrystalline olivine. *J. Geophys. Res.* 107. doi:10.1029/2001JB001225.
- Jackson, I., Webb, S., Weston, L., Boness, D., 2005. Frequency dependence of elastic wave speeds at high temperature: a direct experimental demonstration. *Phys. Earth Planet. Inter.* 148, 85–96.
- Kanamori, H., Anderson, D., 1977. Importance of physical dispersion in surface wave and free oscillation problems: review. *Rev. Geophys. Space Phys.* 15, 105–112.
- Karato, S.I., Spetzler, H., 1990. Defect microdynamics in minerals and solid-state mechanics of seismic wave attenuation and velocity dispersion in the mantle. *Rev. Geophys.* 28, 399–429.
- Kennett, B.L.N., Engdahl, E.R., Buland, R., 1995. Constraints on seismic velocities in the Earth from traveltimes. *Geophys. J. Int.* 122, 108–124.
- Liu, H.P., Anderson, D., Kanamori, H., 1976. Velocity dispersion due to anelasticity: implications for seismology and mantle composition. *Geophys. J. R. Astr. Soc.* 47, 41–58.
- Masters, G., Gilbert, F., 1983. Attenuation in the Earth at low frequencies. *Phil. Trans. R. Soc. Lond.* 308, 479–522.
- Masters, G., Gubbins, D., 2003. On the resolution of density within the Earth. *Phys. Earth Planet. Inter.* 140, 159–167.
- Masters, G., Laske, G., 1997. On bias in surface wave and free oscillation attenuation 681 measurements. *EOS Trans. Am. Geophys. Union* 78, F485.
- Matas, J., Bukowinski, M.S.T., 2007. On the anelastic contribution to the temperature dependence of lower mantle seismic velocities. *Earth Planet. Sci. Lett.* 10.1016/j.epsl.2007.04.028.
- Minster, B., Anderson, D., 1981. A model of dislocation-controlled rheology for the mantle. *Phil. Trans. R. Soc. Lond.* 299, 319–356.
- Ricard, Y., Richards, M., Lithgow-Bertelloni, C., Stunff, Y.L., 1993. A geodynamic model of mantle density heterogeneity. *J. Geophys. Res.* 98, 21895–21910.
- Richards, M.A., Hager, B.H., 1984. Geoid anomalies in a dynamic earth. *J. Geophys. Res.* 89, 5987–6002.
- Romanowicz, B., 1990. The upper mantle degree 2: constraints and inference from global mantle wave attenuation measurements. *J. Geophys. Res.* 95, 11051–11071.
- Romanowicz, B., 1994. Anelastic tomography: a new perspective on upper mantle thermal structure. *Earth Planet. Sci. Lett.* 128, 113–121.
- Romanowicz, B., Mitchell, B., 2007. Deep Earth structure:  $Q$  of the Earth from crust to core. In: Schubert, G. (Ed.), *Treatise on Geophysics*, 1. Elsevier, pp. 731–774.
- Roult, G., Clévéd, E., 2000. New refinements in attenuation measurements from free-oscillation and surface-wave observations. *Phys. Earth Planet. Inter.* 121, 1–2.
- Selby, N.D., Woodhouse, J.H., 2002. The  $Q$  structure of the upper mantle: constraints from Rayleigh wave amplitudes. *J. Geophys. Res.* 107, 5–1.
- Shito, A., Karato, S.I., Park, J., 2004. Frequency dependence of  $Q$  in Earth's upper mantle inferred from continuous spectra of body waves. *Geophys. Res. Lett.* 31. doi:10.1029/2004GL019582.
- Sipkin, S., Jordan, T., 1979. Frequency dependence of  $Q_{scs}$ . *Bull. Seismol. Soc. Am.* 69, 1055–1079.
- Smith, M., Dahlen, F., 1981. The period and  $Q$  of the Chandler wobble. *Geophys. J. R. Astr. Soc.* 64, 223–281.
- Ulug, A., Berckhemer, H., 1984. Frequency dependence of  $Q$  for seismic body waves in the Earth's mantle. *J. Geophys.* 56, 9–19.
- Widmer, R., Masters, G., Gilbert, F., 1991. Spherically symmetric attenuation within the Earth from normal mode data. *Geophys. J. Int.* 104, 541–553.
- Woodhouse, J.H., 1998. The calculation of eigenfrequencies and eigenfunctions of the free oscillations of the Earth and the Sun. In: Doornbos, D. (Ed.), *Seismological Algorithms*. Elsevier, New York, pp. 321–370.